



## Driving mechanism of a failed eruption

Y. Guo<sup>1,2\*</sup>, M. D. Ding<sup>1,2</sup>, B. Schmieder<sup>3</sup>, H. Li<sup>4</sup>, T. Török<sup>5</sup> and  
T. Wiegmann<sup>6</sup>

<sup>1</sup>Department of Astronomy, Nanjing University, Nanjing 210093, China

<sup>2</sup>Key Laboratory for Modern Astronomy and Astrophysics (Nanjing University),  
Ministry of Education, Nanjing 210093, China

<sup>3</sup>Observatoire de Paris, Section de Meudon, LESIA, 92195 Meudon Principal Cedex, France

<sup>4</sup>Purple Mountain Observatory, 2 West Beijing Road, Nanjing 210008, China

<sup>5</sup>Predictive Science, Inc., 9990 Mesa Rim Road, Suite 170, San Diego, CA 92121

<sup>6</sup>Max-Planck-Institut für Sonnensystemforschung, Max-Planck-Strasse 2,  
37191 Katlenburg-Lindau, Germany

**Abstract.** We find a magnetic flux rope before the M1.1 flare in active region 10767 on 2005 May 27 by a nonlinear force-free field extrapolation. *TRACE* observations of the filament eruption show that the erupting structure performed a writhing deformation and stopped rising at a certain height, suggesting that the flux rope converted some of its twist into writhe and was confined in the corona. After calculating the twist of the flux rope, we find that it was comparable to thresholds of the helical kink instability found in numerical simulations. We conclude that the activation and rise of the flux rope were triggered and initially driven by the kink instability. The decay index of the external magnetic field stays below the threshold for the torus instability within a long height range. The confinement of the eruption could be explained by the failure of the torus instability. Hard X-ray sources at the peak of the M1.1 flare coincided with the footpoints of the erupting helical structure, which indicates a high possibility that hard X-ray sources were produced more efficiently in the flux rope.

**Keywords :** Sun: corona – Sun: filaments, prominences – Sun: flares

---

\*email: guoyang@nju.edu.cn

## 1. Introduction

Flux rope eruptions play a key role in various activities on the Sun, such as filament eruptions, coronal mass ejections (CMEs), and flares. The free energy for a flux rope eruption comes from the electric currents contained in the twisted magnetic field lines. The kink instability is the most unstable mode in such a field configuration. An flux rope eruption due to the kink instability displays a writhing deformation of its axis. Since many erupting prominences perform such a deformation, the kink instability has been proposed as the mechanism to trigger and initially drive the eruption (Sakurai 1976; Török & Kliem 2005). The onset condition of the kink instability mainly depends on the total twist of a flux rope. By considering arched flux rope models that are line-tied on the photosphere, Fan & Gibson (2003) and Török, Kliem & Titov (2004) found critical twist values of  $3.0\pi$  and  $3.5\pi$ , respectively. Additionally, the critical twist depends on the twist profile along the flux rope radius and the ratio between the radius and the axis pitch length (Baty 2001).

Although the kink instability can drive an eruption initially, there is no evidence showing that it could drive a full eruption, namely a CME. Theoretical models for accelerating a CME focus on the loss of equilibrium (Forbes & Isenberg 1991) or the torus instability (Kliem & Török 2006). In the loss of equilibrium model, a line current is inserted in the corona, which is constrained by the magnetic tension of the external background field. An image current is introduced below the photosphere to simulate the rigid boundary of the photosphere due to its high inertia. Thus, the repulsion force generated by the two line currents balances the magnetic tension downward. The equilibrium can be broken down by either the increase of electric current or the decrease of magnetic tension. The loss of equilibrium ejects the flux rope upwards and stretches the overlying field lines, which forms a current sheet just below the line current.

When the current path in the corona is deformed to shapes other than a straight line, especially to a semicircle, a Lorentz self force will be present due to the poloidal magnetic field generated by the electric current. This force points from the inner center of the current ring to the outside. Kliem & Török (2006) studied the expansion instability of a toroidal current ring. It is found that if the external poloidal magnetic field  $B_{\text{ex}}$  decreases fast enough along its major radius  $R$ , such as  $-\partial \ln B_{\text{ex}} / \partial \ln R > 3/2$ , an instability occurs, which is termed as the torus instability. Démoulin & Aulanier (2010) pointed out that the loss of equilibrium and the stability analysis are two different views of the same physical mechanism and the repulsion forces working in both the straight line current and the circular current have the same origin.

Sometimes, a flux rope eruption could be confined in the corona and does not lead to a CME, which is termed as a failed eruption (e.g., Ji et al. 2003). Guo et al. (2010a) found a magnetic flux rope coexisting with magnetic arcades about two hours before the M1.1 flare in active region 10767 on 2005 May 27. Guo et al. (2010b) found that the flux rope erupted finally to generate the M1.1 flare, but the eruption

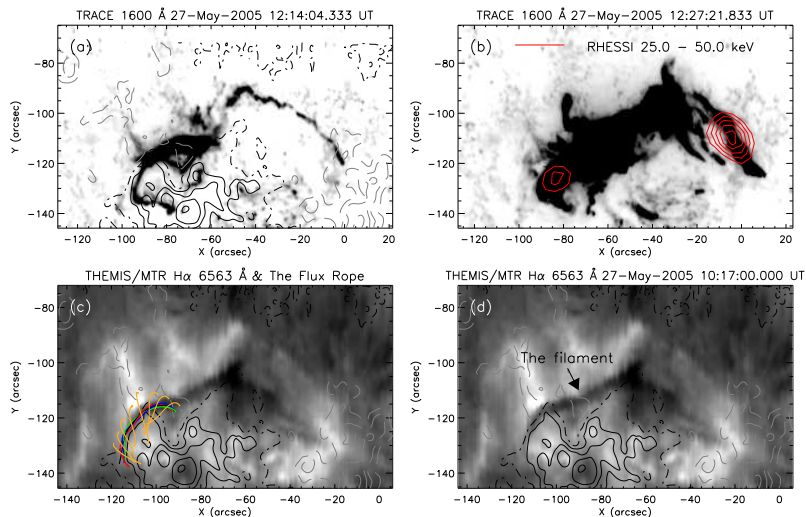


**Figure 1.** (a) *TRACE* 1600 Å image at 12:14 UT on 2005 May 27 (the scale is reversed). Solid, dashed, and dash-dotted contours denote positive polarity, negative polarity, and the polarity inversion line, respectively. The magnetic field was observed by *THEMIS*/MTR. (b) *TRACE* 1600 Å image at 12:27 UT. Contours denote the hard X-ray source observed by *RHESSI*. (c) Magnetic flux rope by nonlinear force-free field extrapolation overlaid on an H $\alpha$  filament. (d) The H $\alpha$  filament was observed by *THEMIS*/MTR in a time range centered at 10:17 UT.

was confined in the corona. In this paper, we will summarize the previous results briefly and study the hard X-ray emissions of this flare. Especially, we have given a more detailed analysis on the twist computation with more extrapolations in different grid resolutions.

## 2. Analysis and results

The M1.1 flare that peaked at about 12:30 UT on 2005 May 27 in the active region NOAA 10767 was fully covered by *TRACE* (Handy et al. 1999) in the 1600 Å band with a cadence of about 30 s. Two *TRACE* 1600 Å images close to the onset time and the peak time are plotted in Fig. 1(a) and (b), respectively. We find that the flare started from the eastern part of the filament, which coincided with the flux rope as shown in Fig. 1(c). However, the final eruption corresponded to the whole filament (Figs 1(b) and 1(d)). These findings suggest that a tether-cutting type magnetic reconnection occurred during the flux rope eruption to form the larger erupting structure at the peak time. The structure showed a helical deformation during the eruption, which is a typical evolution behavior in the kink instability. The apex of the erupting structure stopped ascending at a certain height. It does not evolve into a CME. We have checked other observations, such as *SOHO*/LASCO (Brueckner et al. 1995). However, this eruption happened close to the solar disk center, a halo CME could be missed by

LASCO C2. Within the limited available data, we found no obvious evidence showing that a CME was associated with this event.

We overlay the contours of the hard X-ray (25–50 keV) source observed by *RHESSI* (Lin et al. 2002) at its peak time (12:27:20–12:27:40 UT) on the *TRACE* 1600 Å image as shown in Fig. 1(b). Due to the Neupert effect, the peak time of the soft X-ray flux (12:30 UT) was more than two minutes later than the peak time of the hard X-ray flux. Fig. 1(b) shows that the hard X-ray sources at the peak of the M1.1 flare coincided with the footpoints of the erupting helical structure. Since the helical structure indicates the existence of a larger flux rope during the eruption, the hard X-ray sources should be generated by high energy electrons accelerated in the flux rope. Only in this way, the electrons could propagate along the field lines to precipitate at the footpoints of the flux rope.

The flux rope as shown in Fig. 1(c) is extrapolated by the nonlinear force-free field model (Wiegmann 2004) using the vector magnetic field observed by *THEMIS/MTR* (Bommier et al. 2007) as the bottom boundary. In order to check if the kink instability could trigger the eruption, we have computed the twist in the flux rope. Please refer to Guo et al. (2010b) for details in determining the axis of the flux rope and the formula for computing the twist of two curves with arbitrary geometries. We define the average twist of some selected field lines as the twist of the whole flux rope. With this requirement, the boundary of the flux rope is also determined, which is approximately those field lines that are tangent with the bottom boundary.

To further test the validity of computing the flux rope twist, we have performed additional extrapolations with different grid resolutions in the  $z$ -direction ( $\Delta z = \Delta x = \Delta y$ ,  $\Delta z = \frac{1}{2}\Delta x = \frac{1}{2}\Delta y$ , and  $\Delta z = \frac{1}{4}\Delta x = \frac{1}{4}\Delta y$ ). The resolution on the bottom boundary always keeps the same. The results show that there are no more grid points to resolve the flux rope when the resolution along the  $z$ -direction is increased. This problem seems to be caused by the boundary conditions. However, all the three extrapolated results reveal the existence of the flux rope. We have also computed the twist of the sample field lines around the axis curve. The twists of field lines that are longer than the axis are plotted in Fig. 2. All the twist values are between about  $2.6\pi$ – $4.0\pi$  in radian (or 1.3–2.0 turns). The average twists of the three cases are  $3.6\pi$ ,  $3.8\pi$ , and  $3.0\pi$ , respectively, which are comparable to the thresholds of the kink instability found in numerical simulations (Fan & Gibson 2003; Török et al. 2004).

We also estimate the height distribution of the decay index of the external magnetic field before the eruption with a potential field. The decay indices stayed below the threshold for the torus instability for a significant height range above the erupting flux rope. The torus instability that accounts for a full eruption was most probably not triggered. The flux rope eruption was constrained in the corona, which explains why there was no CME associated with this event. We should take this explanation with caution, since both the external field used in our analysis and the threshold derived from analytical solutions or numerical simulations have appropriate approximations.

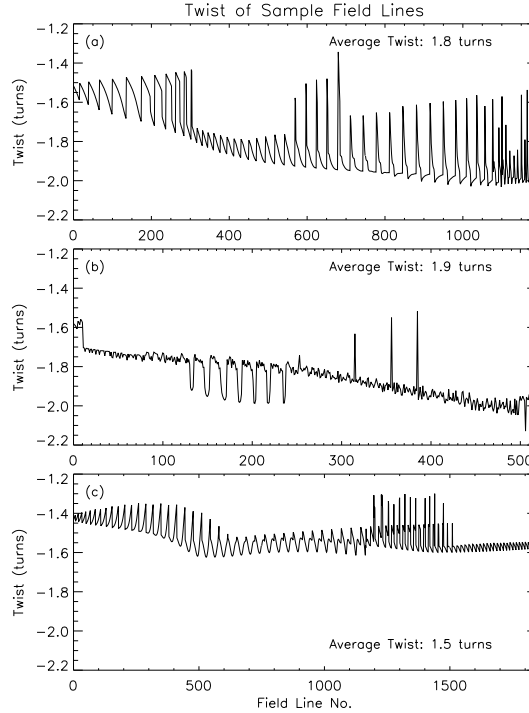


**Figure 2.** Twist numbers of the flux rope computed by extrapolation results with different grid resolutions in the  $z$ -direction. The resolution on the bottom boundary always keeps the same. (a)  $\Delta z = \Delta x = \Delta y$ . (b)  $\Delta z = \frac{1}{2}\Delta x = \frac{1}{2}\Delta y$ . (c)  $\Delta z = \frac{1}{4}\Delta x = \frac{1}{4}\Delta y$ .

### 3. Summary and discussions

We have found a flux rope corresponding to the eastern part of an  $H\alpha$  filament by the nonlinear force-free field extrapolation, and the western part was associated with magnetic arcades (Guo et al. 2010a). The whole filament erupted about two hours after the time of the extrapolated flux rope. Since the erupting helical structure displayed a writhing deformation, we conclude that the kink instability triggered and initially drove the eruption (Guo et al. 2010b). The twists of the extrapolated flux rope in different grid resolutions were comparable to the threshold found by numerical simulations, which supports the idea that the kink instability triggered and initially drove the eruption. However, a full eruption needs the onset of the torus instability, which did not occur in the event, since the external magnetic field did not decay fast enough along the height.

We find that hard X-ray sources at the peak of the M1.1 flare coincided with the footpoints of the erupting helical structure, which suggests that the high energy

electrons are mostly accelerated in the flux rope. Török et al. (2004) found that the erupting flux rope due to kink instability could form two current systems, one is a helical current sheet at the interface of flux rope with the surrounding magnetic fluid, and the other is vertical current sheet below it. In our case, the magnetic reconnection in the former current sheets seems to accelerate particles more efficiently.

With cylindrical flux ropes, Baty (2001) pointed out that the critical twist for the kink instability is close to  $2.5\pi$  if  $r_0/l_0 \gg 1$  ( $r_0$  and  $l_0$  are the radius and axis pitch length of a flux rope, respectively), however, the critical twist sharply increases as  $r_0/l_0 \leq 1$ . The axis pitch length  $l_0 = L/\Phi(0)$ , where  $\Phi(r) = (LB_\theta)/(rB_z)$ ,  $L$  is the flux rope length,  $B_\theta$  and  $B_z$  are the azimuthal and axial components of the magnetic field. If the twist density does not change along the radius  $r$ ,  $r_0/l_0 \approx B_\theta(r_0)/B_z(r_0)$ . We have found that  $B_\theta(r_0) < B_z(r_0)$  in Guo et al. (2010a), therefore,  $r_0/l_0 < 1$  in our case and the critical twist should be much higher than  $2.5\pi$ . Two reasons may account for the occurrence of the kink instability. First, the flare started about two hours after the time of the extrapolated flux rope. During this period, the flux rope might have grown larger via magnetic reconnection. Secondly, the surrounding magnetic field of the flux rope is not potential, but becomes slowly less sheared with the radius. Therefore, the kink instability could occur even though we only get the twist numbers of  $3.6\pi$ ,  $3.8\pi$ , and  $3.0\pi$  in the extrapolations with different grid resolutions.

### Acknowledgements

We are grateful to the *THEMIS*, *TRACE*, *SOHO*, and *RHESSI* teams for providing the valuable data. Y.G. and M.D.D. are supported by NSFC under grants 10828306 and 10933003, and by NKBRFSF under grant 2011CB811402. B.S. is supported by the FP7 program (2007-2013) under grant 218816 (SOTERIA project, [www.soteria-space.eu](http://www.soteria-space.eu)). B.S. also would like to thank ISSI workshop team managed by Klaus Gaalsgardon emerging magnetic flux for interesting discussions on flux tubes. H.L. is supported by NSFC under grants 10873038 and 10833007. T.T. is supported by the NASA HTP and LWS programs. T.W. is supported by DLR-grant 50 OC 0501.

### References

- Baty H., 2001, *A&A*, 367, 321  
 Bommier V. et al., 2007, *A&A*, 464, 323  
 Brueckner G. E. et al., 1995, *Solar Phys.*, 162, 357  
 Démoulin P., Aulanier G., 2010, *ApJ*, 718, 1388  
 Fan Y., Gibson, S. E., 2003, *ApJ*, 589, L105  
 Forbes T. G., Isenberg P. A., 1991, *ApJ*, 373, 294  
 Guo Y. et al., 2010a, *ApJ*, 714, 343  
 Guo Y. et al., 2010b, *ApJ*, 725, L38  
 Handy B. N. et al., 1999, *Solar Phys.*, 187, 229

- Ji H. et al., 2003, *ApJ*, 595, L135  
Kliem B., Török T., 2006, *Phys. Rev. Lett.*, 96, 255002  
Lin R. P. et al., 2002, *Solar Phys.*, 210, 3  
Sakurai T., 1976, *PASJ*, 28, 177  
Török T., Kliem B., 2005, *ApJ*, 630, L97  
Török T., Kliem B., Titov V. S., 2004, *A&A*, 413, L27  
Wiegmann T., 2004, *Solar Phys.*, 219, 87